

MambAttention: Mamba with Multi-Head Attention for Generalizable Single-Channel Speech Enhancement

Nikolai Lund Kühne, *Graduate Student Member, IEEE*, Jesper Jensen, *Member, IEEE*, Jan Østergaard, *Senior Member, IEEE*, and Zheng-Hua Tan, *Senior Member, IEEE*

Abstract—With the advent of new sequence models like Mamba and xLSTM, several studies have shown that these models match or outperform state-of-the-art models in single-channel speech enhancement, automatic speech recognition, and self-supervised audio representation learning. However, prior research has demonstrated that sequence models like LSTM and Mamba tend to overfit to the training set. To address this issue, previous works have shown that adding self-attention to LSTMs substantially improves generalization performance for single-channel speech enhancement. Nevertheless, neither the concept of hybrid Mamba and time-frequency attention models nor their generalization performance have been explored for speech enhancement. In this paper, we propose a novel hybrid architecture, MambAttention, which combines Mamba and shared time- and frequency-multi-head attention modules for generalizable single-channel speech enhancement. To train our model, we introduce VoiceBank+Demand Extended (VB-DemandEx), a dataset inspired by VoiceBank+Demand but with more challenging noise types and lower signal-to-noise ratios. Trained on VB-DemandEx, our proposed MambAttention model significantly outperforms existing state-of-the-art LSTM-, xLSTM-, Mamba-, and Conformer-based systems of similar complexity across all reported metrics on two out-of-domain datasets: DNS 2020 and EARS-WHAM_v2, while matching their performance on the in-domain dataset VB-DemandEx. Ablation studies highlight the role of weight sharing between the time- and frequency-multi-head attention modules for generalization performance. Finally, we explore integrating the shared time- and frequency-multi-head attention modules with LSTM and xLSTM, which yields a notable performance improvement on the out-of-domain datasets. However, our MambAttention model remains superior on both out-of-domain datasets across all reported evaluation metrics.

Index Terms—Attention mechanism, deep learning architecture, generalizable speech enhancement, Mamba, xLSTM.

I. INTRODUCTION

SPEECH enhancement aims to improve the speech intelligibility and speech quality of noisy speech signals, by removing background noise and recovering the desired speech

This work has been submitted to the IEEE for possible publication. Copyright may be transferred without notice, after which this version may no longer be accessible.

This work was supported by the Danish e-Infrastructure Consortium (DeiC) by enabling access to the LUMI supercomputer (g.a. DeiC-AAU-N5-2025126-“Exploring new neural architectures for deep learning based speech enhancement”).

This work is partially supported by the William Demant Fonden via the Centre for Acoustic Signal Processing Research (CASPR).

Nikolai Lund Kühne, Jan Østergaard, and Zheng-Hua Tan are with the Department of Electronic Systems, Aalborg University, 9220, Denmark (e-mail: nlk@es.aau.dk; jo@es.aau.dk; zt@es.aau.dk). Zheng-Hua Tan is also with the Pioneer Centre for AI, 1350, Denmark.

Jesper Jensen is with the Department of Electronic Systems, Aalborg University, 9220, Denmark, and also with Oticon A/S, 2765, Denmark (e-mail: jesj@demant.com).

signal. It is a widely studied subject, since speech enhancement is both challenging and has a wide array of applications such as hearing assistive devices, mobile communication devices, speech recognition systems, and speaker verification systems.

Over the last decade, research on the single-microphone setting, also known as single-channel speech enhancement, has developed from using classical signal-processing techniques such as Kalman filtering [1], subspace approaches [2], and Minimum Mean Square Error Short-Time Spectral Amplitude estimation [3]–[5] to using deep neural networks (DNNs) [6], [7]. As the field of deep learning evolves, new neural architectures emerge. This has led to a large selection of deep learning-based single-channel speech enhancement systems using a variety of neural architectures such as deep denoising autoencoders [8], recurrent neural networks (RNNs) and Long Short-Term Memory (LSTMs) networks [9], [10], convolutional neural networks (CNNs) [11]–[13], diffusion models [14]–[17], generative adversarial networks (GANs) [18]–[22], and state-space models (SSMs) [23]–[25]. With the advent of the Transformer [26], attention-based speech enhancement systems have dominated the field, achieving state-of-the-art on several datasets [27], [28].

However, scaled dot-product attention-based models like Transformers and Conformers [29] scale poorly with sequence length and require large training datasets [30], [31]. Hence, recent works have focused on newly proposed sequence models with linear scalability with respect to sequence length such as Mamba [32] and Extended Long Short-Term Memory (xLSTM) [33]. Mamba and xLSTM have already shown great promise in natural language processing (NLP) [32], [33], computer vision [34], [35], and self-supervised audio representation learning [36], [37]. Additionally, Mamba and xLSTM have recently been shown to match or outperform state-of-the-art speech enhancement systems [38], [39]. On the other hand, [39] also found that a correctly configured LSTM-based model can actually match Conformer-, Mamba-, and xLSTM-based systems on the VoiceBank+Demand dataset [40], [41]. However, most papers reporting state-of-the-art often only evaluate in-domain speech enhancement performance. Arguably, in-domain speech enhancement performance may not be representative of performance in real-world environments, where speech and noise signals may vary significantly from the training data. For this reason, we focus on developing a speech enhancement algorithm that yields superior cross-corpus generalization performance.

Prior works found that LSTMs overfit to the training dataset for automatic speech recognition in recurrent neural network transducers (RNN-T), which results in poor generalization per-

formance [42], [43]. To remedy this, [42] combines multiple regularization techniques during training, and uses dynamic overlapping inference by segmenting long utterances into multiple fixed-length segments, which are decoded independently. On the other hand, [43] proposes using sparse self-attention layers in the Conformer RNN-T. Additionally, they hypothesize that during inference on long utterances, unseen linguistic context can accumulate excessively in the hidden state of the LSTM. They found that resetting the hidden states at silent segments can help mitigate this. Similarly, [44] hypothesizes that domain-specific information can potentially be accumulated or even amplified in hidden states during propagation in the Mamba architecture, thus resulting in worse generalization performance. To mitigate this, they propose hidden state suppressing, which reduces the gap between hidden states across domains, and find that this improves generalization performance in image recognition [44].

Instead of focusing on the generalization performance of specific neural architectures, other works focus on the datasets themselves. In [45], it was established that poor generalization performance of speech enhancement DNNs stems from different recording conditions between datasets. It is revealed that the content of a corpus is more important than its size for speech enhancement generalization performance. Finally, it is shown that simply using a smaller frame shift in the short-time Fourier transform (STFT) significantly improves generalization performance. In [46], a generalization assessment framework is presented. The framework accounts for the potential change in the difficulty of the speech enhancement task across datasets. Using this framework, it was found that for a feed-forward neural network (FFNN), two CNNs and an attention-based model, performance degrades the most in speech mismatches. Notably, it was revealed that while the most recent models displayed the best in-domain speech enhancement performance, their out-of-domain speech enhancement performance was beaten by the FFNN-based system [46].

Combining Mamba blocks with Transformer or attention blocks has already shown great promise in NLP [47], [48], where the proposed models match or outperform state-of-the-art models on multiple benchmarks. However, the large token contexts used in NLP prevent the use of self-attention and Multi-Head Attention (MHA). Similarly, combining a Transformer encoder with an SSM results in state-of-the-art performance in automatic speech recognition (ASR) [49]. Beyond NLP and ASR, a hybrid Mamba and MHA model DeFT-Mamba [50] was recently proposed for universal audio separation in multichannel polyphonic scenarios. By combining a gated convolution block (GCB) with a hybrid Mamba and MHA block across frequency- and time-dimensions to capture local frequency-time relations and position-wise global relations, DeFT-Mamba demonstrates state-of-the-art performance in multichannel separation. In [51], Transformer and Mamba layers were combined in a U-Net architecture called TRAMBA. TRAMBA outperforms existing models in practical speech super resolution and enhancement on mobile and wearable platforms in a self-supervised setting. Finally, [45] showed that augmenting an RNN with a self-attention block and a feedforward block substantially improves speech

enhancement performance on out-of-domain datasets.

In this paper, we propose a novel hybrid Mamba and MHA model (MambAttention) for generalizable single-channel speech enhancement. MambAttention comprises both time- and frequency-Mamba and MHA modules. As opposed to [47]–[49], the time- and frequency-MHA modules in our MambAttention model are placed before their respective time- and frequency-Mamba blocks. Additionally, in contrast to DeFT-Mamba [50], our MambAttention model - developed independently - processes the encoded input along the time-dimension before the frequency-dimension. As we will demonstrate, this ordering yields superior in- and out-of-domain speech enhancement performance. Moreover, while DeFT-Mamba employs a GCB to shift features by one frequency bin or one time frame before applying the MHA and Mamba blocks to process across frequency or time, our model does not use a GCB. More importantly, our MambAttention model shares weights between the MHA modules within each layer, which sets it apart from most existing hybrid attention models [47]–[52]. By sharing the weights between the MHA modules in each layer, our MambAttention model jointly attends to both time and frequency features. We find that this substantially improves generalization across speakers and noise types. To the best of our knowledge, MambAttention is the first model to combine Mamba with MHA across time and frequency for speech enhancement.

While *VoiceBank+Demand* [40], [41] is a widely-used benchmark for single-channel speech enhancement, the test set contains neither babble noise nor speech-shaped noise (SSN) and the signal-to-noise ratios (SNRs) of both training and test files are not lower than 0 dB. This means speech enhancement systems trained and tested only on *VoiceBank+Demand* are neither exposed to nor evaluated in difficult listening conditions. Motivated by this, we propose a new benchmark: *VoiceBank+Demand Extended (VB-DemandEx)*. Compared to the *VoiceBank+Demand* dataset, our *VB-DemandEx* comprises much lower signal-to-noise ratios and a larger variety of noise types. To evaluate the performance of MambAttention, we train our models on the *VB-DemandEx* training set, and test on the in-domain *VB-DemandEx* test set as well as two out-of-domain test sets from *DNS 2020* [53] and *EARS-WHAM_v2* [54]. Results show that our MambAttention model significantly outperforms existing state-of-the-art LSTM-, xLSTM-, Mamba-, and Conformer-based systems on the out-of-domain test sets across all reported evaluation metrics, while still delivering state-of-the-art performance on the in-domain test set. Ablation studies on our proposed MambAttention model shows that the weight sharing mechanism positively impacts generalization performance. Additionally, we find that placing the MHA modules before the Mamba blocks significantly improves generalization performance. Furthermore, we find that augmenting existing LSTM-, and xLSTM-based speech enhancement systems with our proposed MHA modules also greatly improves generalization performance; however, our MambAttention model remains superior across all datasets and reported evaluation metrics.

To gain further insights, we visualize the latent features of our MambAttention model, and the LSTM-, xLSTM-

, Mamba-, and Conformer-based models. This reveals that after being processed by our MambAttention model and the attention-based Conformer model, the in-domain and out-of-domain samples appear much closer to each other compared to the attention-free LSTM, xLSTM, and Mamba models. This suggests that MHA encourages the model to learn dataset-invariant representations. Finally, our MambAttention model shows superior scalability with respect to dataset size when trained on the large-scale *DNS 2020* dataset, as it outperforms the LSTM, xLSTM, Mamba, and Conformer baselines across all reported metrics. Our major contributions are summarized as follows:

- We propose a novel state-of-the-art hybrid MambAttention model combining Mamba and MHA for generalizable single-channel speech enhancement.
- We propose the *VB-DemandEx* benchmark, which is inspired by *VoiceBank+Demand*, but features substantially lower SNRs and more noise types.
- We demonstrate that weight sharing between time- and frequency-MHA modules in our MambAttention model contributes to its state-of-art generalization performance.
- We show that combining our shared time- and frequency-MHA modules with LSTM- and xLSTM-based models significantly improves their generalization performance.

Code, audio samples, model weights, and the proposed dataset are publicly available.¹

II. PROPOSED METHOD

A. State-Space Models and Mamba

Structured SSMs [55] and Mamba [32] are a family of sequence-to-sequence models inspired by continuous linear time-invariant (LTI) systems. SSMs map an input $x(t) \in \mathbb{R}$ to an output $y(t) \in \mathbb{R}$ through a latent state $\mathbf{h}(t) \in \mathbb{R}^{N \times 1}$ via an evolution parameter $\mathbf{A} \in \mathbb{R}^{N \times N}$, and projection parameters $\mathbf{B} \in \mathbb{R}^{N \times 1}$ and $\mathbf{C} \in \mathbb{R}^{1 \times N}$:

$$\mathbf{h}'(t) = \mathbf{A}\mathbf{h}(t) + \mathbf{B}x(t), \quad (1)$$

$$y(t) = \mathbf{C}\mathbf{h}(t), \quad (2)$$

where $\mathbf{h}'(t) \in \mathbb{R}^{N \times 1}$. To make SSMs applicable in deep neural networks, a time-scale parameter $\Delta \in \mathbb{R}$ is introduced to transform \mathbf{A} and \mathbf{B} into their discrete-time counterparts $\bar{\mathbf{A}} \in \mathbb{R}^{N \times N}$ and $\bar{\mathbf{B}} \in \mathbb{R}^{N \times 1}$ via a zero-order hold [56]:

$$\bar{\mathbf{A}} = \exp(\Delta\mathbf{A}), \quad (3)$$

$$\bar{\mathbf{B}} = (\Delta\mathbf{A})^{-1}(\exp(\Delta\mathbf{A}) - \mathbf{I}) \cdot \Delta\mathbf{B} \approx \Delta\mathbf{B}. \quad (4)$$

The approximation in (4) holds when Δ is small. Thus, the discrete-time versions of (1) and (2) become [32]:

$$\mathbf{h}_i = \bar{\mathbf{A}}\mathbf{h}_{i-1} + \bar{\mathbf{B}}x_i, \quad (5)$$

$$y_i = \mathbf{C}\mathbf{h}_i, \quad (6)$$

where the subscript i is the discrete-time index. Mamba improves upon structured SSMs, by making \mathbf{B} , \mathbf{C} , Δ functions of the input, resulting in the input-dependent parameters $\mathbf{B}_i \in \mathbb{R}^{N \times 1}$, $\mathbf{C}_i \in \mathbb{R}^{1 \times N}$, and $\Delta_i \in \mathbb{R}$. Consequently,

the discretized $\bar{\mathbf{A}}_i = \exp(\Delta_i\mathbf{A})$, $\bar{\mathbf{B}}_i = \Delta_i\mathbf{B}_i$ also become input-dependent. Additionally, Mamba sets \mathbf{A} and $\bar{\mathbf{A}}_i$ as diagonal; hence, defining the vector composed of diagonal elements of $\bar{\mathbf{A}}_i$ as $\tilde{\mathbf{A}}_i = \text{diag}(\bar{\mathbf{A}}_i) \in \mathbb{R}^{N \times 1}$ results in $\bar{\mathbf{A}}_i\mathbf{h}_{i-1} = \tilde{\mathbf{A}}_i \odot \mathbf{h}_{i-1}$, where \odot is element-wise multiplication. Moreover, we can write $\bar{\mathbf{B}}_i x_i = \Delta_i \mathbf{B}_i x_i = \mathbf{B}_i (\Delta_i \odot x_i)$ [56]. Thus, (5) and (6) become:

$$\mathbf{h}_i = \tilde{\mathbf{A}}_i \odot \mathbf{h}_{i-1} + \mathbf{B}_i (\Delta_i \odot x_i), \quad (7)$$

$$y_i = \mathbf{C}_i \mathbf{h}_i, \quad (8)$$

where $x_i, y_i \in \mathbb{R}$, and $\mathbf{h}_i \in \mathbb{R}^{N \times 1}$.

Finally, to operate over an input $\mathbf{X} = [\mathbf{x}_1, \mathbf{x}_2, \dots, \mathbf{x}_L]^\top \in \mathbb{R}^{L \times K}$, where each $\mathbf{x}_i \in \mathbb{R}^{1 \times K}$, Mamba applies (7) and (8) independently to each channel K . Thus, the formulation of Mamba becomes [56]:

$$\mathbf{h}_i = \tilde{\mathbf{A}}_i \odot \mathbf{h}_{i-1} + \mathbf{B}_i (\Delta_i \odot \mathbf{x}_i), \quad (9)$$

$$\mathbf{y}_i = \mathbf{C}_i \mathbf{h}_i, \quad (10)$$

where $\Delta_i \in \mathbb{R}^{1 \times K}$, $\mathbf{B}_i \in \mathbb{R}^{N \times 1}$, $\mathbf{C}_i \in \mathbb{R}^{1 \times N}$ are derived from the input, $\tilde{\mathbf{A}}_i, \mathbf{h}_i \in \mathbb{R}^{N \times K}$, and $\mathbf{y}_i \in \mathbb{R}^{1 \times K}$. In Mamba, the parameters $\mathbf{B} \in \mathbb{R}^{N \times L}$, $\mathbf{C} \in \mathbb{R}^{L \times N}$, and $\Delta \in \mathbb{R}^{L \times K}$ are learned through projections $\mathbf{B} = (\mathbf{X}\mathbf{W}_B)^\top$, $\mathbf{C} = \mathbf{X}\mathbf{W}_C$, and $\Delta = \text{Softplus}(\mathbf{X}\mathbf{W}_1\mathbf{W}_2)$, where $\mathbf{W}_B, \mathbf{W}_C \in \mathbb{R}^{K \times N}$, $\mathbf{W}_1 \in \mathbb{R}^{K \times K_0}$, and $\mathbf{W}_2 \in \mathbb{R}^{K_0 \times K}$ are learnable weight matrices [56], \mathbf{X} is the input, and the Softplus function is defined in [57].

B. Multi-Head Attention

Attention can be interpreted as a vector of importance weights assigned to different parts of the input or output based on context derived from learnable feature spaces [26]. Self-attention is an attention mechanism relating different positions of the same input sequence by assigning different weights to different parts of the input sequence [26]. Informally, an attention mechanism is a mapping of a query and a set of key-value pairs to an output. The popular scaled dot-product attention mechanism is defined as [26]:

$$\text{Attention}(\mathbf{Q}, \mathbf{K}, \mathbf{V}) = \text{Softmax}\left(\frac{\mathbf{Q}\mathbf{K}^\top}{\sqrt{d_k}}\right)\mathbf{V}, \quad (11)$$

where $\mathbf{Q} \in \mathbb{R}^{L \times d_k}$, $\mathbf{K} \in \mathbb{R}^{L \times d_k}$ and $\mathbf{V} \in \mathbb{R}^{L \times d_v}$ is the query, key, and value matrix, respectively, and L is the input sequence length. The query, key, and value matrices are learned projections of the input $\mathbf{X} \in \mathbb{R}^{L \times d_m}$ to their respective dimensions and d_m is the model's feature dimension. In a single self-attention computation, all information from the input is averaged. However, in the MHA mechanism proposed in [26], scaled dot-product attention is computed across h attention heads of dimensionality $\frac{d_m}{h} = d_k = d_v$ in parallel. This allows neural networks utilizing MHA to jointly attend to information from different subspace representations at different positions, meaning that different attention heads capture different information. Given $\mathbf{Q}, \mathbf{K}, \mathbf{V} \in \mathbb{R}^{L \times d_m}$, the MHA mechanism is given by:

$$\text{MHA}(\mathbf{Q}, \mathbf{K}, \mathbf{V}) = \text{Concat}(\text{head}_1, \dots, \text{head}_h)\mathbf{W}^O, \quad (12)$$

$$\text{head}_i = \text{Attention}(\mathbf{Q}\mathbf{W}_i^Q, \mathbf{K}\mathbf{W}_i^K, \mathbf{V}\mathbf{W}_i^V), \quad (13)$$

¹<https://github.com/NikolaiKyhne/MambAttention>

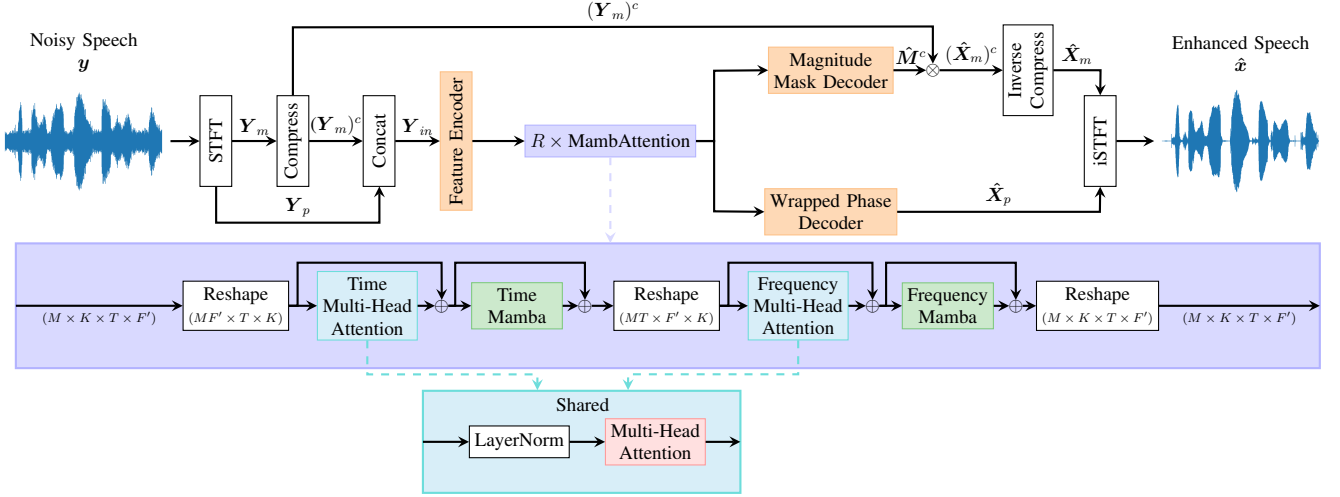


Fig. 1: Overall structure of our proposed MambAttention model. M , K , T , and F' represent the batch size, the number of channels, the number of time frames, and the number of frequency bins, respectively.

where $\text{Concat}(\cdot)$ is the concatenation operation, $\mathbf{W}_i^Q, \mathbf{W}_i^K \in \mathbb{R}^{d_m \times d_k}$, and $\mathbf{W}_i^V \in \mathbb{R}^{d_m \times d_v}$ are learnable weight matrices, $\text{head}_i \in \mathbb{R}^{L \times \frac{d_m}{h}}$ denotes the i th attention head, and $i \in \{1, 2, \dots, h\}$. Finally, $\mathbf{W}^O \in \mathbb{R}^{hd_v \times d_m}$ is the output weight matrix, learning the contribution of each attention head.

C. MambAttention: Mamba with Multi-Head Attention

To improve generalization performance for speech enhancement, we propose the MambAttention block, which is a novel architectural component integrating shared MHA modules with Mamba. Figure 1 illustrates our proposed MambAttention block. Each block jointly models temporal and spectral dependencies, enabling the network to capture complex structures in speech signals. In each MambAttention block, the input $\mathbf{X} \in \mathbb{R}^{M \times K \times T \times F}$ is first reshaped to $MF \times T \times K$ before applying a Layer Normalization (LN), a time-MHA (T-MHA) block and a bidirectional time-Mamba (T-Mamba) block. Here M , K , T , and F represent the batch size, the number of channels, the number of time frames, and the number of frequency bins, respectively. Subsequently, the output of the T-Mamba block is reshaped to $MT \times F \times K$ before another LN, a frequency-MHA (F-MHA) block, and a bidirectional frequency-Mamba (F-Mamba) block is applied. Finally, the output is reshaped back to $M \times K \times T \times F$. Mathematically, given an input \mathbf{X} , the forward pass of a MambAttention block is given by:

$$\mathbf{X}_{\text{Time}} = \text{reshape}(\mathbf{X}, [M \cdot F, T, K]), \quad (14)$$

$$\mathbf{X}_1 = \mathbf{X}_{\text{Time}} + \text{T-MHA}(\text{LN}(\mathbf{X}_{\text{Time}})), \quad (15)$$

$$\mathbf{X}_2 = \mathbf{X}_1 + \text{T-Mamba}(\mathbf{X}_1), \quad (16)$$

$$\mathbf{X}_{\text{Freq.}} = \text{reshape}(\mathbf{X}_2, [M \cdot T, F, K]), \quad (17)$$

$$\mathbf{X}_3 = \mathbf{X}_{\text{Freq.}} + \text{F-MHA}(\text{LN}(\mathbf{X}_{\text{Freq.}})), \quad (18)$$

$$\mathbf{X}_4 = \mathbf{X}_3 + \text{F-Mamba}(\mathbf{X}_3), \quad (19)$$

$$\mathbf{Y} = \text{reshape}(\mathbf{X}_4, [M, K, T, F]), \quad (20)$$

where $\text{reshape}(\text{input}, \text{size})$ reshapes the input to a given size. The T- and F-MHA modules only have one input, since the

queries, keys, and values are all derived from the input. We use the T- and F-Mamba blocks from SEMamba [38], hence the output \mathbf{X}_{out} of each T- and F-Mamba block is given by:

$$\mathbf{X}_{\text{out}} = \text{Conv1D}(\text{Concat}(\text{Mamba}(\mathbf{X}_{\text{in}}), \text{flip}(\text{Mamba}(\text{flip}(\mathbf{X}_{\text{in}}))))), \quad (21)$$

where \mathbf{X}_{in} is the input to the T- and F-Mamba blocks, and $\text{Mamba}(\cdot)$, $\text{flip}(\cdot)$, and $\text{Conv1D}(\cdot)$ is the unidirectional Mamba, the sequence flipping operation, and the 1-D transposed convolution across either time or frequency.

A key element of our MambAttention block is the use of shared weights between the T- and F-MHA modules within each MambAttention block. This weight sharing mechanism allows each layer of the model to simultaneously attend to both time and frequency content. Importantly, as we shall see, weight sharing substantially improves the model's ability to generalize across recording conditions, speaker, and noise types. Finally, weight sharing minimizes the increase in model size and memory cost from adding the MHA modules, resulting in more efficient training.

III. EXPERIMENTAL SETUP

A. Datasets

To generate our proposed *VB-DemandEx* dataset, we use the same clean speech data as *VoiceBank+Demand* [40], [41], but we leave out speakers “p282” (female) and “p287” (male) for validation, as the original *VoiceBank+Demand* benchmark contains no validation set. Like *VoiceBank+Demand*, speakers “p232” and “p257” are used for the test set, and the remaining 26 speakers are used for training. All audio clips are downsampled to 16 kHz. For noise, we use the 16 kHz version of the Demand database [41], which comprises 6 noise categories: Domestic, Office, Public, Transportation, Street, and Nature. In each category, there are 3 subsets of noise recordings. Each subset of noise recordings contains 16 audio signals that are 15 minutes long, enumerated from 1 to 16. In *VoiceBank+Demand*, only selected subsets of each noise

category are present in the training and test sets. To ensure our speech enhancement systems are trained on a bigger variety of noise types, we adopt a different approach. For each subset of noise recordings, we divide the signals into 3 groups of 1-12, 13-14 and 15-16, and concatenate them into training, validation and test splits, respectively. This ensures no shared realizations of noise types between the training, validation, and test sets. The subsets of each noise categories are concatenated further in order to create the splits of 6 different noise types (e.g. $\text{Public_training} = \text{Concat}(\text{PSTATION}[1 - 12], \text{PCAFETER}[1 - 12], \text{PRESTO}[1 - 12])$). In addition to the Demand database, we use babble noise and SSN, which is generated using LibriSpeech [58] as a source, in the training, validation, and test sets. Babble noise is produced by averaging the waveforms of 6 energy-standardized speech signals with silence detected by rVAD [59] being removed, resulting in a single babble signal. To create the SSN, audio signals from selected speakers undergo a 12th order Linear Predictive Coding analysis, yielding coefficient for a all-pole filter that is applied to Gaussian white noise. The train, validation, and test set in *VB-DemandEx*, are generated by sequentially mixing the clean speech and noise at 7 segmental SNRs (SSNRs) [60] ($[-10, -5, 0, 5, 10, 15, 20]$ dB), using the officially provided script from the *Deep Noise Suppression Challenge 2020* [53] (*DNS 2020*). This ensures a uniform distribution of both noise types and SNRs. This results in 10,842 audio clips for training, 730 for validation, and 826 for testing.

Besides training and testing on our proposed *VB-DemandEx* dataset, we also train and test our models on the large-scale *DNS 2020* dataset [53]. This dataset contains 500 hours of clean audio clips from 2,150 speakers and over 180 hours of noise audio clips. Since the original *DNS 2020* dataset contains no validation set, we set aside female speakers “reader_01326”, “reader_06709”, “reader_08788” and male speakers “reader_01105”, “reader_05375”, “reader_11980”, as well as a suitable amount of noise audio clips for validation. Following the officially provided script, the remaining clean and noisy audio clips are used to generate 3,000 hours of noisy-clean pairs of audio clips with SSNRs ranging from -5 dB to 15 dB for training, resulting in 1.08 M 10 s noisy audio clips. We generate the validation set using the same script resulting in 315 10 s audio clips with SSNRs between -5 dB and 15 dB, ensuring a uniform distribution of noise types and SNRs. For evaluation, we use the *DNS 2020* test set without reverberation, which contains 150 noisy-clean pairs generated from audio clips spoken by 20 speakers.

We also test the generalization performance of our models on the 16 kHz version of the *EARS-WHAM_v2* dataset [54], [61]. The dataset comprises clean audio clips from 107 speakers. The clean speech, which is recorded in an anechoic chamber, covers a large variety of speaking styles, including reading tasks in 7 different reading styles, emotional reading and freeform speech in 22 different emotions, as well as conversational speech [54]. Speakers *p001* to *p099* are used for training, *p100* and *p101* are used for validation, and *p102* to *p107* are used for testing. Using the officially provided script [54], the clean speech is mixed with real noise recordings from the *WHAM!* dataset [61] at SNRs randomly sampled between

$[-2.5, 17.5]$ dB. The SNRs are computed using loudness K-weighted relative to full scale, which is standardized in ITU-R BS.1770 [62]. This results in 32,485 noisy-clean pairs for training, 632 noisy-clean pairs for validation, and 886 noisy-clean pairs for testing. The *EARS-WHAM_v2* test set contains utterances up to 29 s in length. Hence, to avoid running out of memory, we perform inference on non-overlapping chunks of 10 s audio clips for all models on the *EARS-WHAM_v2* test set.

B. Model Overview

To be able to directly compare the generalization performance of our MambAttention block with other neural architectures, we integrate it into the widely-used state-of-the-art dual-path system used in MP-SENet [27] (Conformer), SEMamba [38] (Mamba), and xLSTM-SENet [39] (xLSTM). Thus, all pre-processing, feature encoding, final decoding, training hyperparameters, and loss functions are equivalent for all models trained and compared in this paper.

Figure 1 illustrates the overall architecture of our MambAttention model. A complex spectrogram of the noisy speech waveform $\mathbf{y} \in \mathbb{R}^D$ is computed via an STFT. The input to the feature encoder $\mathbf{Y}_{in} \in \mathbb{R}^{T \times F \times 2}$ is the compressed magnitude spectrum $(\mathbf{Y}_m)^c \in \mathbb{R}^{T \times F}$ extracted via power-law compression [63] concatenated with the wrapped phase spectrum $\mathbf{Y}_p \in \mathbb{R}^{T \times F}$. The feature encoder contains two convolution blocks sandwiching a dilated DenseNet [64]. Each convolution block consists of a 2D convolutional layer, an instance normalization, and a PReLU activation [65]. The feature encoder increases the number of input channels from 2 to K and halves the frequency dimension from F to $F' = F/2$.

The output of the feature encoder is then processed by R MambAttention blocks. It is subsequently fed into the magnitude mask decoder and the wrapped phase decoder that predicts the clean compressed magnitude mask $\hat{\mathbf{M}}^c = (\hat{\mathbf{X}}_m / \mathbf{Y}_m)^c \in \mathbb{R}^{T \times F}$ and the clean wrapped phase spectrum $\hat{\mathbf{X}}_p \in \mathbb{R}^{T \times F}$, respectively. The enhanced magnitude spectrum $\hat{\mathbf{X}}_m \in \mathbb{R}^{T \times F}$ is computed as:

$$\hat{\mathbf{X}}_m = ((\mathbf{Y}_m)^c \odot \hat{\mathbf{M}}^c)^{1/c}, \quad (22)$$

where $\hat{\mathbf{M}}^c$ denotes the predicted clean compressed magnitude mask. The magnitude mask decoder comprises a dilated DenseNet, a 2D transposed convolution, an instance normalization, and a PReLU activation. This is followed by a deconvolution block reducing the amount of channels from K to 1, and a learnable sigmoid function with $\beta = 2$ [21] estimating the magnitude mask. Similarly, the wrapped phase decoder consists of a dilated DenseNet, a 2D transposed convolution, an instance normalization, and a PReLU activation. This is followed by two parallel 2D convolutional layers predicting the pseudo-real and pseudo-imaginary part components. The clean wrapped phase spectrum is predicted using the two-argument arctangent function [27], yielding the enhanced wrapped phase spectrum $\hat{\mathbf{X}}_p$. The final enhanced waveform $\hat{\mathbf{x}} \in \mathbb{R}^D$ is recovered by applying an iSTFT to the enhanced magnitude spectrum $\hat{\mathbf{X}}_m$ and the enhanced wrapped phase spectrum $\hat{\mathbf{X}}_p$.

C. Loss Functions

We follow [27], [38], [39] and use a linear combination of loss functions. We use a time loss $\mathcal{L}_{\text{Time}}$, magnitude loss $\mathcal{L}_{\text{Mag.}}$, and complex loss $\mathcal{L}_{\text{Com.}}$ defined by:

$$\mathcal{L}_{\text{Time}} = \mathbb{E}_{\mathbf{x}, \hat{\mathbf{x}}} [\|\mathbf{x} - \hat{\mathbf{x}}\|_1], \quad (23)$$

$$\mathcal{L}_{\text{Mag.}} = \mathbb{E}_{\mathbf{X}_m, \hat{\mathbf{X}}_m} [\|\mathbf{X}_m - \hat{\mathbf{X}}_m\|_2^2], \quad (24)$$

$$\mathcal{L}_{\text{Com.}} = \mathbb{E}_{\mathbf{X}_r, \hat{\mathbf{X}}_r} [\|\mathbf{X}_r - \hat{\mathbf{X}}_r\|_2^2] + \mathbb{E}_{\mathbf{X}_i, \hat{\mathbf{X}}_i} [\|\mathbf{X}_i - \hat{\mathbf{X}}_i\|_2^2], \quad (25)$$

where $\mathbb{E}[\cdot]$ is the expectation operator, $\mathbf{x} \in \mathbb{R}^D$ is the clean speech, $\hat{\mathbf{x}} \in \mathbb{R}^D$ is the enhanced speech, and the pairs $(\mathbf{X}_r, \mathbf{X}_i)$ and $(\hat{\mathbf{X}}_r, \hat{\mathbf{X}}_i)$ are the real and imaginary parts of the clean complex spectrum $\mathbf{X} = \mathbf{X}_m \cdot e^{j\mathbf{X}_p} \in \mathbb{C}^{T \times F}$ and the enhanced complex spectrum $\hat{\mathbf{X}} = \hat{\mathbf{X}}_m \cdot e^{j\hat{\mathbf{X}}_p} \in \mathbb{C}^{T \times F}$, respectively. Additionally, we use the instantaneous phase loss \mathcal{L}_{IP} , group delay loss \mathcal{L}_{GD} , and instantaneous angular frequency loss \mathcal{L}_{IAF} presented in [66] and define the phase loss as:

$$\mathcal{L}_{\text{Pha.}} = \mathcal{L}_{\text{IP}} + \mathcal{L}_{\text{GD}} + \mathcal{L}_{\text{IAF}}. \quad (26)$$

To improve training stability, we employ the consistency loss $\mathcal{L}_{\text{Con.}}$ presented in [67]:

$$\mathcal{L}_{\text{Con.}} = \mathbb{E}_{\hat{\mathbf{X}}_r} [\|\hat{\mathbf{X}}_r - \text{STFT}(\text{iSTFT}(\hat{\mathbf{X}}_r))\|_2^2] + \mathbb{E}_{\hat{\mathbf{X}}_i} [\|\hat{\mathbf{X}}_i - \text{STFT}(\text{iSTFT}(\hat{\mathbf{X}}_i))\|_2^2]. \quad (27)$$

Finally, we use the metric discriminator D from [22] for adversarial training, which uses perceptual evaluation of speech quality (PESQ) as the target objective metric. The PESQ scores are linearly normalized to $[0, 1]$. The discriminator loss \mathcal{L}_{D} and its corresponding PESQ-based generator loss $\mathcal{L}_{\text{PESQ}}$ are given by:

$$\mathcal{L}_{\text{D}} = \mathbb{E}_{\mathbf{X}_m} [\|D(\mathbf{X}_m, \mathbf{X}_m) - 1\|_2^2] + \mathbb{E}_{\mathbf{X}_m, \hat{\mathbf{X}}_m} [\|D(\mathbf{X}_m, \hat{\mathbf{X}}_m) - Q_{\text{PESQ}}\|_2^2], \quad (28)$$

and

$$\mathcal{L}_{\text{PESQ}} = \mathbb{E}_{\mathbf{X}_m, \hat{\mathbf{X}}_m} [\|D(\mathbf{X}_m, \hat{\mathbf{X}}_m) - 1\|_2^2], \quad (29)$$

where $Q_{\text{PESQ}} \in [0, 1]$ is the scaled PESQ score between \mathbf{X}_m and $\hat{\mathbf{X}}_m$. The final generator loss \mathcal{L}_{G} then becomes a linear combination of the above-mentioned loss functions:

$$\mathcal{L}_{\text{G}} = \alpha_1 \mathcal{L}_{\text{Time}} + \alpha_2 \mathcal{L}_{\text{Mag.}} + \alpha_3 \mathcal{L}_{\text{Com.}} + \alpha_4 \mathcal{L}_{\text{Pha.}} + \alpha_5 \mathcal{L}_{\text{Con.}} + \alpha_6 \mathcal{L}_{\text{PESQ}}. \quad (30)$$

During training, \mathcal{L}_{G} and \mathcal{L}_{D} are jointly minimized.

D. Hyperparameter Settings

To reduce training time and vRAM usage, we follow [27], [38], [39] and train all models on randomly cropped 2s audio clips. Unless audio files are natively sampled at 16 kHz, they are downsampled to 16 kHz. We use an FFT order of 400, a Hann window size of 400, and a hop size of 100 for all STFTs. Moreover, we use a magnitude spectrum compression factor of $c = 0.3$ [27]. For Conformer [27], Mamba [38], xLSTM [39], and our MambAttention model, we fix the model

feature dimension and number of channels $d_m = K = 64$, the amount of layers $R = 4$, and the expansion factor to $E_f = 4$. As there are no pre- or post-up projections in the LSTM model, we follow [39] and double the amount of layers to $R = 8$ and maintain the model feature dimension and number of channels $d_m = K = 64$ to approximately match the parameter count of the Conformer, Mamba, and xLSTM models. In the Conformer and our proposed MambAttention model, we use $h = 8$ attention heads. We follow [28], and set the hyperparameters in the generator loss function to $\alpha_1 = 0.2, \alpha_2 = 0.9, \alpha_3 = 0.1, \alpha_4 = 0.3, \alpha_5 = 0.1$, and $\alpha_6 = 0.05$. All models trained on *VB-DemandEx* and *DNS 2020* are trained for 550k and 950k steps respectively, with a batch size of $M = 8$ on four AMD MI250X GPUs, as validation performance stops improving when training longer. For both the generator and discriminator, we use AdamW [68] with an initial learning rate of 0.0005, a weight decay of 0.01, $\beta_1 = 0.8$, and $\beta_2 = 0.99$. We use an exponential learning rate scheduler with a learning rate decay of 0.99. For evaluation, we select the checkpoint with the highest PESQ score on the validation set, saved every 250 steps.

E. Evaluation Metrics

Here, we describe the standard speech enhancement metrics for assessing the performance of our proposed method.

To assess the quality of the enhanced speech, we apply wide-band PESQ [69], which reports values between -0.5 (poor) and 4.5 (excellent). Additionally, we report the standard waveform-matching-based evaluation metrics SSNR [60] and scale-invariant signal-to-distortion ratio (SI-SDR) [70]. Both SSNR and SI-SDR are reported in dB. To predict the intelligibility of the enhanced speech, we use extended short-time objective intelligibility (ESTOI) [71], which effectively reports values between 0 and 1. For all measures, higher values indicate better performance. All models are trained with 5 different seeds, and we report the mean and standard deviation.

IV. RESULTS

In this section, we present the results of our proposed MambAttention model for speech enhancement. First, we present the speech enhancement performance on our proposed *VB-DemandEx* dataset, and compare with existing state-of-the-art baselines. Simultaneously, we assess generalization performance on the out-of-domain *DNS 2020* and *EARS-WHAM_v2* test sets. Then, we present an ablation study of our proposed MambAttention model. We also investigate integrating MHA with other neural architectures, and compare their in- and out-of-domain speech enhancement performance to our proposed MambAttention block. Finally, we visually inspect latent features produced by our proposed MambAttention model and baselines, and we report results when training on the large-scale *DNS 2020* dataset.

A. Generalization Performance

To assess the generalization performance of our proposed MambAttention model, we train and evaluate on our *VB-*

TABLE I: In-domain and out-of-domain speech enhancement performance. Models are trained and *VB-DemandEx*.

Dataset	Params (M)	In-Domain				Out-Of-Domain							
		<i>VB-DemandEx</i>				<i>DNS 2020</i>				<i>EARS-WHAM_v2</i>			
		PESQ	SSNR	ESTOI	SI-SDR	PESQ	SSNR	ESTOI	SI-SDR	PESQ	SSNR	ESTOI	SI-SDR
Noisy	-	1.625	-1.068	0.630	4.976	1.582	6.218	0.810	9.071	1.235	-0.803	0.640	5.359
xLSTM [39]	2.20	2.973±0.051	7.933±0.133	0.795±0.008	16.414±0.317	1.724±0.368	3.246±1.332	0.686±0.097	3.412±3.482	1.505±0.151	0.446±0.566	0.559±0.053	1.396±2.141
LSTM [39]	2.34	3.002±0.026	7.981±0.210	0.802±0.003	16.637±0.123	1.984±0.454	4.901±1.656	0.724±0.117	4.749±3.346	1.570±0.179	0.854±0.773	0.566±0.083	1.916±2.894
Mamba [38]	2.25	3.002±0.022	7.590±0.177	0.800±0.003	16.593±0.159	2.281±0.134	5.837±1.033	0.820±0.028	9.298±1.576	1.631±0.053	0.921±0.508	0.603±0.026	2.809±0.523
Conformer [27]	2.05	2.935±0.065	7.641±0.283	0.787±0.010	16.202±0.318	2.666±0.010	7.369±0.382	0.875±0.009	13.665±0.892	1.862±0.097	2.107±0.270	0.677±0.029	6.090±0.672
MambAttention	2.33	3.026±0.007	7.674±0.411	0.801±0.002	16.684±0.095	2.919±0.118	8.133±0.733	0.911±0.009	15.169±1.363	2.010±0.053	2.505±0.224	0.725±0.020	7.348±0.445

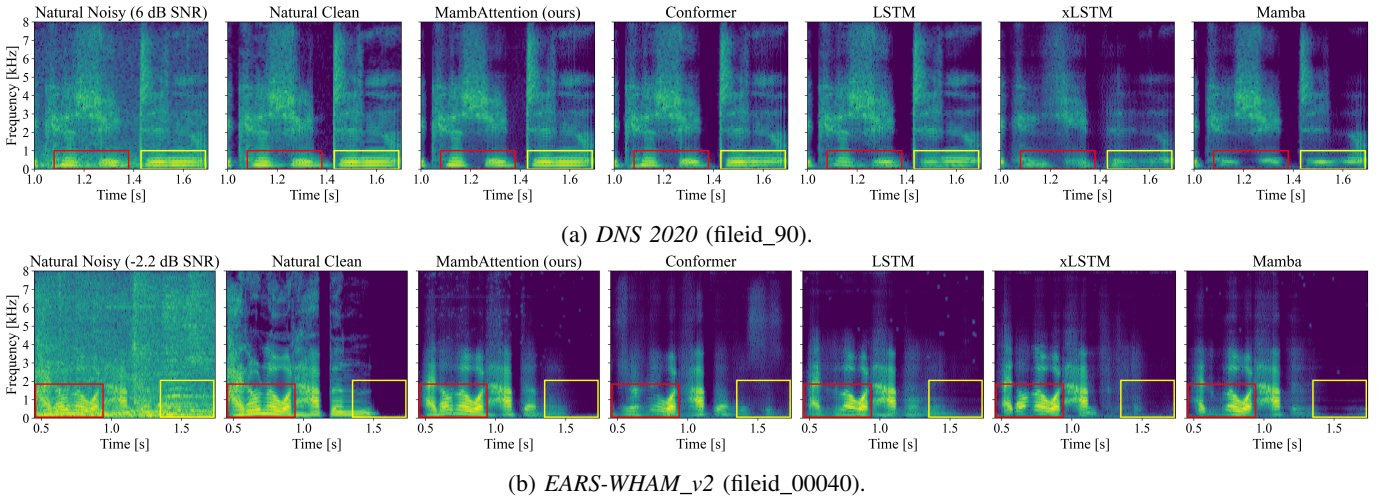


Fig. 2: Spectrogram visualizations of the noisy speech, clean speech, and enhanced speech from our proposed MambAttention and the Conformer, LSTM, xLSTM, and Mamba baselines.

DemandEx dataset. We also evaluate on two very different out-of-domain test sets from *DNS 2020* and *EARS-WHAM_v2*. In Table I, we report in- and out-of-domain speech enhancement performance of our MambAttention model as well as state-of-the-art LSTM-, xLSTM-, Mamba-, and Conformer-based baselines [27], [38], [39].

We observe that our proposed MambAttention model outperforms all other models on the out-of-domain datasets on all reported metrics. This indicates superior generalization performance compared to existing models, as both recording conditions, noise, and speaker types are significantly different across both out-of-domain datasets compared to our *VB-DemandEx* dataset. Compared to the Mamba-based model from [38], we remark that adding the shared MHA modules greatly improves out-of-domain performance, while only adding approximately 3.4% additional parameters. For example, on *DNS 2020*, PESQ increases by 0.638, SSNR increases by 2.296, ESTOI increases by 0.091, and SI-SDR increases by 5.871 from using our MambAttention model over the pure Mamba baseline. Moreover, we observe that the recurrent sequence models LSTM and xLSTM exhibit the worst generalization performance, which could indicate overfitting to the training set, or domain-specific information being accumulated in the hidden state as hypothesized in [43], [44]. In fact, both LSTM and xLSTM yield worse SSNR, ESTOI, and SI-SDR scores on the out-of-domain *DNS 2020* test set than the unprocessed noisy samples from the *DNS 2020* test set. Mamba, while still being a sequence model, shows substantially better generalization performance compared to

LSTM and xLSTM; however, only the attention-based Conformer and our MambAttention model consistently improve all reported metrics on both out-of-domain datasets. Additionally, we observe that all models exhibit comparable performance on the in-domain *VB-DemandEx* dataset. This aligns with previous findings on the *VoiceBank+Demand* dataset, which features higher SNRs compared to *VB-DemandEx* [39].

To support the claim of superior generalization performance of our MambAttention model, we visualize spectrograms of clean speech, noisy speech, and the speech waveforms enhanced by our MambAttention model and the LSTM, xLSTM, Mamba, and Conformer baselines on the out-of-domain *DNS 2020* and *EARS-WHAM_v2* test sets. For each model in Figure 2, we select the seed with the median PESQ score on each test set to provide a fair comparison. As seen in the yellow and red boxes in Figure 2a, our MambAttention model and the Conformer-based model are the only models that mostly reconstruct the fundamental harmonics. The red boxes in Figure 2b reveal the same effect at a significantly lower SNR, but to a larger extent. Interestingly, the yellow boxes in Figure 2b show that only our MambAttention model, and to some extent, the xLSTM- and Mamba-based baselines, almost reconstruct silence, whereas the Conformer- and LSTM-based baselines do not.

B. Ablation Study

To investigate the performance impact of key architectural design choices, we conduct ablation studies on the shared MHA modules in our MambAttention block. Specifically,

TABLE II: Ablation study. Default configurations for our MambAttention model are the T- and F-MHA modules before the T- and F-Mamba blocks, respectively, shared weights between the T- and F-MHA modules, and processing across the time-dimension before the frequency-dimension. Models are trained on *VB-DemandEx*.

Dataset	Params (M)	In-Domain				Out-Of-Domain							
		<i>VB-DemandEx</i>				<i>DNS 2020</i>				<i>EARS-WHAM_v2</i>			
		PESQ	SSNR	ESTOI	SI-SDR	PESQ	SSNR	ESTOI	SI-SDR	PESQ	SSNR	ESTOI	SI-SDR
Noisy	-	1.625	-1.068	0.630	4.976	1.582	6.218	0.810	9.071	1.235	-0.803	0.640	5.359
MambAttention	2.33	3.026±0.007	7.674±0.411	0.801±0.002	16.684±0.095	2.919±0.118	8.133±0.733	0.911±0.009	15.169±1.363	2.010±0.053	2.505±0.224	0.725±0.020	7.348±0.445
Attention after	2.33	3.031±0.008	7.765±0.161	0.804±0.001	16.712±0.062	2.706±0.202	7.229±0.984	0.870±0.032	12.859±2.303	1.927±0.136	1.704±0.371	0.678±0.048	4.835±0.694
w/o weight sharing	2.39	3.039±0.010	7.954±0.068	0.803±0.001	16.713±0.095	2.610±0.233	6.755±1.231	0.856±0.052	11.575±2.706	1.878±0.066	1.605±0.319	0.672±0.016	4.449±0.996
w/o MHA modules [38]	2.25	3.002±0.022	7.590±0.177	0.800±0.003	16.593±0.159	2.281±0.134	5.837±1.033	0.820±0.028	9.298±1.576	1.631±0.053	0.921±0.508	0.603±0.026	2.809±0.523
Frequency → Time	2.33	3.021±0.029	7.650±0.203	0.800±0.007	16.573±0.172	2.545±0.395	6.270±1.398	0.843±0.071	11.280±4.250	1.846±0.244	1.532±0.801	0.648±0.088	4.300±3.368

TABLE III: In-domain and out-of-domain speech enhancement performance of LSTM- and xLSTM-based models with added MHA modules. Models are trained on *VB-DemandEx*.

Dataset	Params (M)	In-Domain				Out-Of-Domain							
		<i>VB-DemandEx</i>				<i>DNS 2020</i>				<i>EARS-WHAM_v2</i>			
		PESQ	SSNR	ESTOI	SI-SDR	PESQ	SSNR	ESTOI	SI-SDR	PESQ	SSNR	ESTOI	SI-SDR
Noisy	-	1.625	-1.068	0.630	4.976	1.582	6.218	0.810	9.071	1.235	-0.803	0.640	5.359
xLSTM-Attention	2.27	3.019±0.010	7.689±0.186	0.800±0.002	16.653±0.107	2.801±0.167	7.187±0.931	0.886±0.025	13.913±1.889	1.927±0.104	1.962±0.381	0.680±0.024	6.144±1.280
LSTM-Attention	2.48	3.023±0.037	7.645±0.339	0.803±0.008	16.596±0.279	2.546±0.183	5.792±0.878	0.847±0.032	10.961±1.622	1.855±0.163	1.168±0.488	0.663±0.056	4.506±1.806
Conformer [27]	2.05	2.935±0.065	7.641±0.283	0.787±0.010	16.202±0.318	2.666±0.010	7.369±0.382	0.875±0.009	13.665±0.892	1.862±0.097	2.107±0.270	0.677±0.029	6.090±0.672
MambAttention	2.33	3.026±0.007	7.674±0.411	0.801±0.002	16.684±0.095	2.919±0.118	8.133±0.733	0.911±0.009	15.169±1.363	2.010±0.053	2.505±0.224	0.725±0.020	7.348±0.445

we change the order of the MHA and Mamba blocks, and we test the effect of using separate trainable parameters for the T- and F-MHA modules instead of shared ones in each MambAttention block. As shown in Table II, reversing the order of the MHA and Mamba blocks, negatively affects generalization performance on both out-of-domain datasets, as all reported performance metrics drop on both out-of-domain test sets. Hence, the ordering of components in our proposed MambAttention block affects the model’s ability to generalize beyond the training distribution. Moreover, assigning separate weights to each T- and F-MHA module slightly increases parameter count but degrades generalization performance. This highlights the importance of the weight sharing mechanism for maintaining robustness to unseen speakers, noise types, and recording conditions. We hypothesize that weight sharing across the T- and F-MHA modules acts as a form of regularization. Instead of each individual MHA module attending to either time or frequency contents, we believe that the shared MHA modules force each layer of our MambAttention model to attend to time and frequency contents simultaneously. Thus, rather than overfitting to dataset-specific features, we believe the shared MHA modules encourage a focus on learning time and frequency structures that are more likely to generalize across various noise and speaker types. We remark that although the ablation studies on the MHA modules in Table II lead to reduced generalization performance, all variants still outperform the pure Mamba baseline from [38]. Additionally, we flip the order of the time and frequency processing components in our MambAttention model. Table II (Frequency → Time) demonstrates that processing along the frequency-dimension before the time-dimension yields significantly worse generalization performance, as all metrics on both out-of-domain test sets decrease significantly. These results align with CMGAN [22], which showed that processing across frequency before time in TS-Conformers yields worse speech enhancement performance.

We also integrate our T- and F-MHA modules into the xLSTM- and LSTM-based speech enhancement models from

[39] and denote them xLSTM-Attention and LSTM-Attention, respectively. For the xLSTM-Attention model, we replace the T and F-Mamba blocks in Figure 1 with the T- and F-xLSTM blocks from [39]. Similarly, for the LSTM-Attention model, we replace the T- and F-Mamba blocks in Figure 1 with the T- and F-LSTM blocks from [39]. Additionally, for the LSTM-Attention model, we reverse the order of the T-MHA and T-LSTM blocks and the order of the F-MHA and F-LSTM blocks, respectively. We choose these configurations for the xLSTM-Attention and LSTM-Attention models, as we found this yields the best generalization performance. We remark that in [52], the attention block was also placed after the LSTM block. In all cases, in-domain performance remains unchanged. As shown in Table III, both LSTM-Attention and xLSTM-Attention significantly outperform their MHA-free counterparts from Table I on the two out-of-domain test sets. The xLSTM-Attention model consistently surpasses the Conformer baseline on the *DNS 2020* and *EARS-WHAM_v2* test sets across all evaluation metrics except SSNR. Despite LSTM-Attention significantly surpassing its MHA-free baseline counterpart, the Conformer baseline remains superior on both out-of-domain test sets across all evaluation metrics used. These results are in line with [52], where self-attending RNNs also were shown to improve cross-corpus generalization performance over their attention-free counterparts. We do, however, observe a significantly larger increase in generalization performance by adding our shared T- and F-MHA modules to the LSTM- and xLSTM-based models compared to [52], which only uses a single self-attention block. Nevertheless, our proposed MambAttention model achieves superior generalization performance compared to both LSTM-Attention and xLSTM-Attention.

C. Inspection of Latent Features

In Table I, we observe that the attention-based Conformer and our MambAttention model demonstrate significantly better generalization performance compared to the purely recurrent LSTM-, xLSTM-, and Mamba-based baselines. This is also

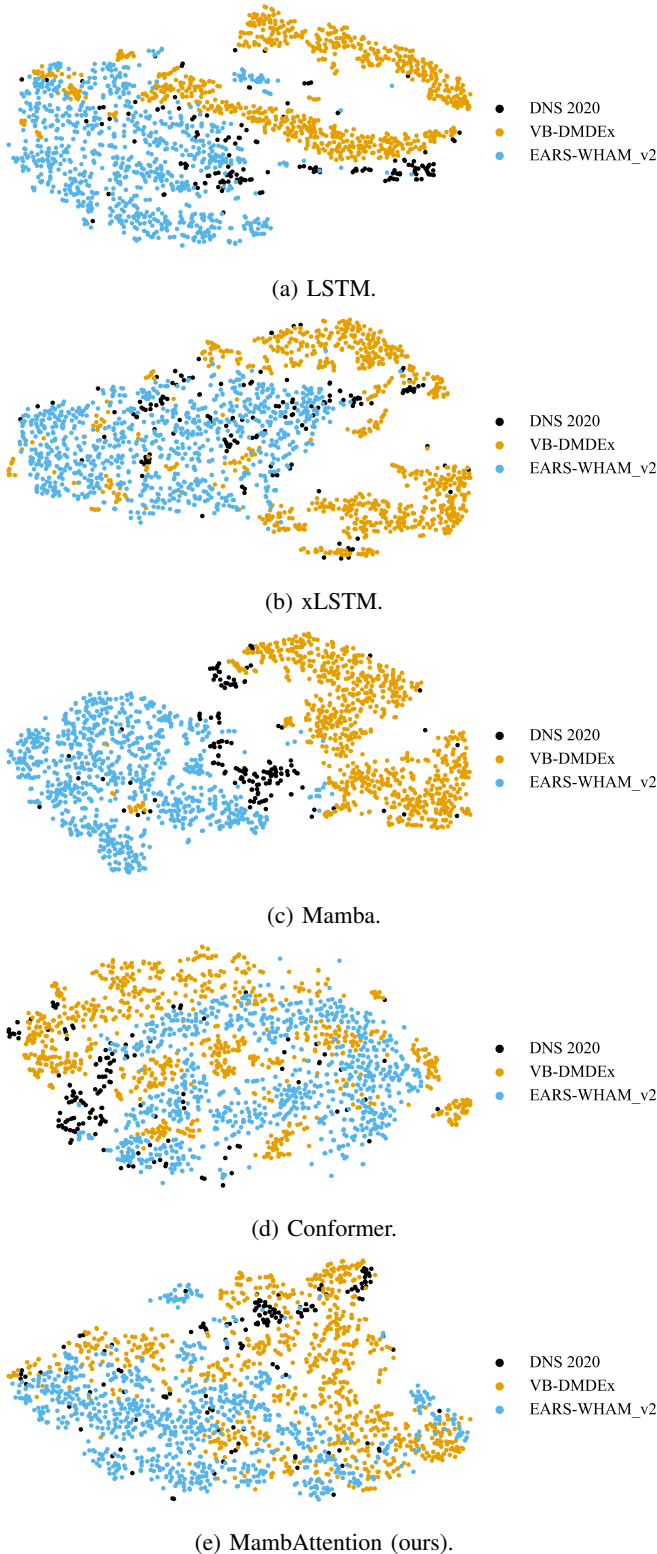


Fig. 3: t-SNE visualizations of the *VB-DemandEx*, *DNS 2020*, and *EARS-WHAM_v2* test sets.

consistently reflected in Table III when comparing attention-augmented baseline models with their attention-free counterparts from Table I. To further understand the impact MHA has on generalization performance, we visually inspect the

latent features produced by the LSTM-, xLSTM-, Mamba-, and Conformer-based models as well as our MambAttention model. Using t-Distributed Stochastic Neighbor Embedding (t-SNE) [72], we visualize the outputs of the final LSTM, xLSTM, Mamba, Conformer, and MambAttention blocks, before they are passed to the magnitude mask and wrapped phase decoders. As we train all models with 5 different seeds, we select the seed with the median PESQ score on the out-of-domain *DNS 2020* test set to provide a fair comparison. The t-SNE visualizations are done on the *VB-DemandEx*, *DNS 2020*, and *EARS-WHAM_v2* test sets.

As shown in Figure 3, the t-SNE embeddings for the in-domain and out-of-domain samples appear less tightly clustered and more intermingled across domains for the attention-based Conformer (Figure 3d) and our MambAttention model (Figure 3e), compared to models with poorer generalization performance: LSTM (Figure 3a), xLSTM (Figure 3b), and Mamba (Figure 3c). For the LSTM, xLSTM, and Mamba models, the t-SNE embeddings of the individual test sets are significantly more clustered. At first sight, Figure 3 may be surprising, however, the features in Figure 3d and Figure 3e show that after being processed by the Conformer or our MambAttention blocks, t-SNE embeddings of both the in-domain and out-of-domain noisy speech are very close. This indicates that the learned features are less dataset-dependent, which supports our claim of superior generalization performance. Furthermore, this suggests that MHA may encourage the model to learn more dataset-invariant representations, rather than overfitting to dataset-specific patterns.

To gain further insights into the effect of the shared MHA modules in our MambAttention model compared to the pure Mamba baseline, we visualize t-SNE embeddings of the in-domain and out-of-domain *VB-DemandEx*, *DNS 2020*, and *EARS-WHAM_v2* test sets along with their clean references in Figure 4. In Figure 4b we observe that after being processed by the MambAttention blocks, the t-SNE embeddings of the in- and out-of-domain clean references are clustered together. Moreover, the noisy speech is very close to their clean references in the t-SNE embedding space, suggesting that processed noisy speech and processed clean speech is similar. This indicates that the denoising process of the MambAttention blocks is effective, supporting the results presented in Table I. This is in stark contrast to the pure Mamba model in Figure 4a, where we observe that the t-SNE embeddings of both noisy speech and clean references are clearly separated and far apart.

D. Results on *DNS 2020*

As shown in Table I, a range of neural architectures, including our proposed MambAttention model, achieve similar in-domain speech enhancement performance on our *VB-DemandEx* dataset. Hence, in order to examine whether increased volume and data diversity better differentiate in-domain model performance, we train on the large-scale *DNS 2020* dataset [53].

TABLE IV: Training time on the *VB-DemandEx* and *DNS 2020* training sets measured in GPU hours (wall clock time \times number of GPUs) and inference time (wall clock time) measured in seconds on the *VB-DemandEx*, *DNS 2020* and *EARS-WHAM_v2* test sets.

Model	Params (M)	FLOPs (G)	Training Time (per dataset)		Inference Time (per dataset)		
			<i>VB-DemandEx</i>	<i>DNS 2020</i>	<i>VB-DemandEx</i>	<i>DNS 2020</i>	<i>EARS-WHAM_v2</i>
xLSTM [39]	2.20	80.71	862 GPU Hours	1499 GPU Hours	142 s	215 s	2580 s
LSTM [39]	2.34	88.59	131 GPU Hours	225 GPU Hours	28 s	37 s	214 s
Mamba [38]	2.25	64.46	187 GPU Hours	325 GPU Hours	36 s	48 s	244 s
Conformer [27]	2.05	74.29	388 GPU Hours	675 GPU Hours	58 s	96 s	790 s
MambAttention	2.33	65.52	212 GPU Hours	365 GPU Hours	43 s	68 s	697 s

TABLE V: Speech Enhancement performance on *DNS 2020*.

Model	Params (M)	PESQ	SSNR	ESTOI	SI-SDR
Noisy	-	1.582	6.218	0.810	9.071
xLSTM [39]	2.20	3.588 \pm 0.017	14.526 \pm 0.482	0.954 \pm 0.001	20.854 \pm 0.226
LSTM [39]	2.34	3.598 \pm 0.031	15.021 \pm 0.168	0.956 \pm 0.002	21.003 \pm 0.215
Mamba [38]	2.25	3.594 \pm 0.012	14.830 \pm 0.473	0.955 \pm 0.001	21.035 \pm 0.123
Conformer [27]	2.05	3.605 \pm 0.021	14.967 \pm 0.044	0.954 \pm 0.000	20.919 \pm 0.021
MambAttention	2.33	3.671 \pm 0.008	15.116 \pm 0.049	0.959 \pm 0.000	21.234 \pm 0.033

Table V shows in-domain speech enhancement performance on the *DNS 2020* dataset. We observe that when trained on *DNS 2020*, compared to the pure Mamba baseline, our MambAttention model yields a PESQ score which is bigger by 0.077 and ESTOI is bigger by 0.004. In contrast, Table I shows that on *VB-DemandEx*, compared to Mamba, MambAttention yields a PESQ score and ESTOI which is bigger by only 0.024, and 0.001, respectively. As all models in Table V have comparable parameter counts, and our MambAttention model also slightly outperforms the baselines across all reported metrics on the *DNS 2020* dataset, we argue that this indicates that our MambAttention model scales more effectively with respect to dataset size. This suggests that our proposed MambAttention block is better suited for leveraging large, diverse training data for speech enhancement tasks.

E. Training and Inference Efficiency

In Table IV, we report training time in GPU hours on the *VB-DemandEx* and *DNS 2020* training sets and inference time in seconds on the *VB-DemandEx*, *DNS 2020*, and *EARS-WHAM_v2* test sets for our MambAttention model and the baselines. As NVIDIA GPUs are more common than AMD GPUs in published AI research, we report training and inference time on NVIDIA GPUs. The training times for each model are reported by training 1 seed on four NVIDIA L40S GPUs, and the inference time is computed by running inference on a single NVIDIA L40S GPU. In addition, we report FLOPs, which are computed based on processing a single 2s audio clip on one GPU.

Table IV shows that training our MambAttention model requires approximately 13% more GPU hours than the Mamba baseline. For inference, we observe that the difference in inference time between the Mamba baseline and our MambAttention model becomes larger on the *EARS-WHAM_v2* test set compared to the *VB-DemandEX* and *DNS 2020* test sets. We attribute this to the fact that the utterances in the

EARS-WHAM_v2 test set are considerably longer. Thus, the quadratic complexity of the MHA modules has a bigger impact on inference time. Our MambAttention model remains significantly more efficient than the Conformer- and xLSTM-based baselines with respect to both training and inference time. As shown in Table IV, our MambAttention model only requires slightly more FLOPs than the Mamba baseline, and it requires less FLOPs than the LSTM, xLSTM, and Conformer baselines.

Since the LSTM-based baseline does not contain any pre-up or post-down projections, as opposed to the xLSTM, Mamba, and MambAttention models, we hypothesize that this is the reason for lower training and inference time.

V. DISCUSSION AND LIMITATIONS

While our MambAttention model displays superior generalization performance for speech enhancement compared to LSTM, xLSTM, Mamba, and Conformer, it does come at a cost. The addition of MHA adds additional trainable parameters, and due to using scaled dot-product attention, we no longer have linear scalability with respect to the input sequence length. This is one of the main advantages of newer sequence models such as Mamba [32] and xLSTM [33]. Hence, Table IV shows an increase in training time by approximately 13% compared to the Mamba baseline. However, as we train on 2s audio clips and run inference on at most 10s chunks of audio clips, the impact of the quadratic complexity of the MHA modules becomes less noticeable. Thus, this may only become an issue for real-time speech enhancement or for processing longer audio clips. To overcome the quadratic complexity of self-attention, recent works have introduced IO-aware exact attention algorithms and approximate methods resulting in significant reductions in runtime [73]–[75]. These algorithms potentially counteract the computational downsides of using MHA.

As observed in Table I, all models perform similar when trained and evaluated on our proposed *VB-DemandEx* dataset. This result is in line with our previous work in [39], where we reported that LSTM-, xLSTM-, Mamba-, and Conformer-based models perform similarly on the *VoiceBank+Demand* dataset [40], [41]. Thus, our results add solid evidence to the conclusions drawn in [39], since our proposed *VB-DemandEx* dataset features substantially lower SNRs and more noise types compared to *VoiceBank+Demand*. The lack of performance differentiation between models, despite differences in noise

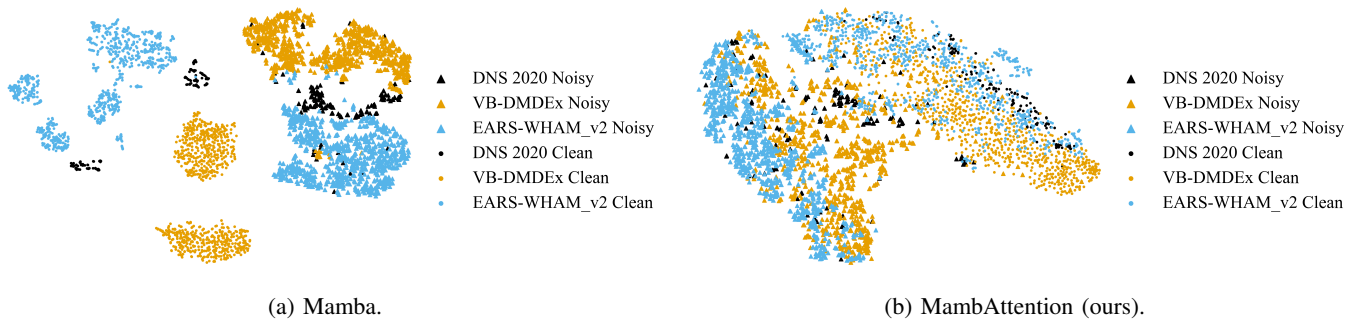


Fig. 4: t-SNE visualizations of the *VB-DemandEx*, *DNS 2020*, and *EARS-WHAM_v2* test sets along with their clean references.

diversity and SNRs across training datasets, raises concerns about solely using such small-scale datasets for benchmarking speech enhancement performance. Thus, exclusively presenting performance on such datasets may obscure differences in model performance that only become apparent on larger and more diverse datasets or in mismatched speaker, noise, and recording conditions as observed in Table V and Table I, respectively.

VI. CONCLUSION

In this paper, we proposed a novel MambAttention model that combines Mamba and shared multi-head attention for generalizable single-channel speech enhancement. To evaluate its performance, we introduced *VB-DemandEx*, a new speech enhancement dataset based on *VoiceBank+Demand* but with lower SNRs and more challenging noise types. When trained on *VB-DemandEx*, our MambAttention model outperforms state-of-the-art LSTM-, xLSTM-, Mamba-, and Conformer-based systems of similar complexity across all reported metrics when evaluating on the two out-of-domain datasets: *DNS 2020* and *EARS-WHAM_v2*, while matching their performance on the in-domain *VB-DemandEx* dataset. Detailed ablation studies reveal that the placement of the multi-head-attention modules significantly affect the generalization performance of our MambAttention model. Additionally, we found that the weight sharing mechanism positively affects generalization performance, while slightly reducing the overall parameter count. We also tested multi-head attention-augmented LSTM and xLSTM variants, which improved their generalization performance but remained inferior to our MambAttention model. Finally, results on the large-scale *DNS 2020* dataset demonstrate that our MambAttention model scales more effectively with dataset size, achieving superior in-domain performance across all reported metrics compared to state-of-the-art LSTM-, xLSTM-, Mamba-, and Conformer-based baselines of similar complexity.

While our MambAttention model outperforms state-of-the-art baselines in generalization performance, exploring real-time performance will be the focus of our future work. This will require an update to the entire MambAttention model, as neither the feature encoder, the time- and frequency-multi-head attention modules, the time- and frequency-Mamba blocks, nor the decoders are causal. However, we believe this would be a feasible research direction, since Mamba- and attention-based

models have already shown potential for real-time speech enhancement [76], [77].

REFERENCES

- [1] K. Paliwal and A. Basu, "A speech enhancement method based on kalman filtering," in *IEEE International Conference on Acoustics, Speech, and Signal Processing*, vol. 12, 1987, pp. 177–180.
- [2] Y. Ephraim and H. L. Van Trees, "A signal subspace approach for speech enhancement," *IEEE Transactions on Speech and Audio Processing*, vol. 3, no. 4, pp. 251–266, 1995.
- [3] Y. Ephraim and D. Malah, "Speech enhancement using a minimum-mean square error short-time spectral amplitude estimator," *IEEE Transactions on Acoustics, Speech, and Signal Processing*, vol. 32, no. 6, 1984.
- [4] D. Griffin and J. Lim, "Signal estimation from modified short-time fourier transform," *IEEE Transactions on Acoustics, Speech, and Signal Processing*, vol. 32, no. 2, pp. 236–243, 1984.
- [5] Y. Ephraim and D. Malah, "Speech enhancement using a minimum mean-square error log-spectral amplitude estimator," *IEEE Transactions on Acoustics, Speech, and Signal Processing*, vol. 33, no. 2, pp. 443–445, 1985.
- [6] Y. Xu, J. Du, L.-R. Dai, and C.-H. Lee, "A regression approach to speech enhancement based on deep neural networks," *IEEE/ACM Transactions on Audio, Speech, and Language Processing*, vol. 23, no. 1, pp. 7–19, 2014.
- [7] M. Kolbæk, Z.-H. Tan, and J. Jensen, "Speech intelligibility potential of general and specialized deep neural network based speech enhancement systems," *IEEE/ACM Transactions on Audio, Speech, and Language Processing*, vol. 25, no. 1, pp. 153–167, 2016.
- [8] X. Lu, Y. Tsao, S. Matsuda, and C. Hori, "Speech enhancement based on deep denoising autoencoder," in *INTERSPEECH*, vol. 2013, 2013, pp. 436–440.
- [9] F. Wening, J. R. Hershey, J. Le Roux, and B. Schuller, "Discriminatively trained recurrent neural networks for single-channel speech separation," in *IEEE global conference on signal and information processing*, 2014, pp. 577–581.
- [10] K. Tesch, N.-H. Mohrmann, and T. Gerkmann, "On the role of spatial, spectral, and temporal processing for dnn-based non-linear multi-channel speech enhancement," in *INTERSPEECH*, 2022, pp. 2908–2912.
- [11] S.-W. Fu, Y. Tsao, X. Lu *et al.*, "Snr-aware convolutional neural network modeling for speech enhancement," in *INTERSPEECH*, 2016, pp. 3768–3772.
- [12] A. Pandey and D. Wang, "A new framework for cnn-based speech enhancement in the time domain," *IEEE/ACM Transactions on Audio, Speech, and Language Processing*, vol. 27, no. 7, pp. 1179–1188, 2019.
- [13] M. Kolbæk, Z.-H. Tan, S. H. Jensen, and J. Jensen, "On loss functions for supervised monaural time-domain speech enhancement," *IEEE/ACM Transactions on Audio, Speech, and Language Processing*, vol. 28, pp. 825–838, 2020.
- [14] Y.-J. Lu, Z.-Q. Wang, S. Watanabe, A. Richard, C. Yu, and Y. Tsao, "Conditional diffusion probabilistic model for speech enhancement," in *IEEE International Conference on Acoustics, Speech, and Signal Processing*, 2022, pp. 7402–7406.
- [15] J. Richter, S. Welker, J.-M. Lemercier, B. Lay, and T. Gerkmann, "Speech enhancement and dereverberation with diffusion-based generative models," *IEEE/ACM Transactions on Audio, Speech, and Language Processing*, vol. 31, pp. 2351–2364, 2023.

- [16] J. Richter, S. Welker, J.-M. Lemerrier, B. Lay, T. Peer, and T. Gerkmann, "Causal diffusion models for generalized speech enhancement," *IEEE Open Journal of Signal Processing*, 2024.
- [17] P. Gonzalez, Z.-H. Tan, J. Østergaard, J. Jensen, T. S. Alstrøm, and T. May, "Investigating the design space of diffusion models for speech enhancement," *IEEE/ACM Transactions on Audio, Speech, and Language Processing*, 2024.
- [18] D. Michelsanti and Z.-H. Tan, "Conditional generative adversarial networks for speech enhancement and noise-robust speaker verification," in *INTERSPEECH*, 2017, pp. 2008–2012.
- [19] S. Pascual, A. Bonafonte, and J. Serrà, "Segan: Speech enhancement generative adversarial network," in *INTERSPEECH*, 2017, pp. 3642–3646.
- [20] S.-W. Fu, C.-F. Liao, Y. Tsao, and S.-D. Lin, "Metricgan: Generative adversarial networks based black-box metric scores optimization for speech enhancement," in *International Conference on Machine Learning*, 2019, pp. 2031–2041.
- [21] S.-W. Fu, C. Yu, T.-A. Hsieh, P. Plantinga, M. Ravanelli, X. Lu, and Y. Tsao, "Metricgan+: An improved version of metricgan for speech enhancement," in *INTERSPEECH*, 2021.
- [22] S. Abdulatif, R. Cao, and B. Yang, "Cmgn: Conformer-based metricgan for monaural speech enhancement," *IEEE/ACM Transactions on Audio, Speech, and Language Processing*, vol. 32, pp. 2477–2493, 2024.
- [23] L. Sun, S. Yuan, A. Gong, L. Ye, and E. S. Chng, "Dual-branch modeling based on state-space model for speech enhancement," *IEEE/ACM Transactions on Audio, Speech, and Language Processing*, vol. 32, pp. 1457–1467, 2024.
- [24] P.-J. Ku, C.-H. H. Yang, S. Siniscalchi, and C.-H. Lee, "A multi-dimensional deep structured state space approach to speech enhancement using small-footprint models," in *INTERSPEECH*, 2023, pp. 2453–2457.
- [25] Y. Du, X. Liu, and Y. Chua, "Spiking structured state space model for monaural speech enhancement," in *IEEE International Conference on Acoustics, Speech and Signal Processing*, 2024, pp. 766–770.
- [26] A. Vaswani, N. Shazeer, N. Parmar, J. Uszkoreit, L. Jones, A. N. Gomez, Ł. Kaiser, and I. Polosukhin, "Attention is all you need," *Advances in Neural Information Processing Systems*, vol. 30, 2017.
- [27] Y.-X. Lu, Y. Ai, and Z.-H. Ling, "Mp-senet: A speech enhancement model with parallel denoising of magnitude and phase spectra," in *INTERSPEECH*, 2023, pp. 3834–3838.
- [28] —, "Explicit estimation of magnitude and phase spectra in parallel for high-quality speech enhancement," *Neural Networks*, vol. 189, p. 107562, 2025.
- [29] A. Gulati, J. Qin, C.-C. Chiu, N. Parmar, Y. Zhang, J. Yu, W. Han, S. Wang, Z. Zhang, Y. Wu, and R. Pang, "Conformer: Convolution-augmented transformer for speech recognition," in *INTERSPEECH*, 2020, pp. 5036–5040.
- [30] D. de Oliveira, T. Peer, and T. Gerkmann, "Efficient transformer-based speech enhancement using long frames and stft magnitudes," in *INTERSPEECH*, 2022, pp. 2948–2952.
- [31] Y. Gong, Y.-A. Chung, and J. Glass, "Ast: Audio spectrogram transformer," in *INTERSPEECH*, 2021, pp. 571–575.
- [32] A. Gu and T. Dao, "Mamba: Linear-time sequence modeling with selective state spaces," in *First Conference on Language Modeling*, 2024.
- [33] M. Beck, K. Pöppel, M. Spanring, A. Auer, O. Prudnikova, M. K. Kopp, G. Klambauer, J. Brandstetter, and S. Hochreiter, "xLSTM: Extended long short-term memory," in *The Thirty-eighth Annual Conference on Neural Information Processing Systems*, 2024.
- [34] L. Zhu, B. Liao, Q. Zhang, X. Wang, W. Liu, and X. Wang, "Vision mamba: Efficient visual representation learning with bidirectional state space model," in *Forty-first International Conference on Machine Learning*, 2024.
- [35] B. Alkin, M. Beck, K. Pöppel, S. Hochreiter, and J. Brandstetter, "Vision-1stm: xlstm as generic vision backbone," in *The Thirteenth International Conference on Learning Representations*, 2025.
- [36] S. Yadav and Z.-H. Tan, "Audio mamba: Selective state spaces for self-supervised audio representations," in *INTERSPEECH*, 2024, pp. 552–556.
- [37] S. Yadav, S. Theodoridis, and Z.-H. Tan, "Audio xlstms: Learning self-supervised audio representations with xlstms," in *INTERSPEECH (Accepted)*, 2025.
- [38] R. Chao, W.-H. Cheng, M. La Quatra, S. M. Siniscalchi, C.-H. H. Yang, S.-W. Fu, and Y. Tsao, "An investigation of incorporating mamba for speech enhancement," in *IEEE Spoken Language Technology Workshop*, 2024, pp. 302–308.
- [39] N. L. Kühne, J. Østergaard, J. Jensen, and Z.-H. Tan, "xLSTM-SENet: xLSTM for Single-Channel Speech Enhancement," in *INTERSPEECH (Accepted)*, 2025.
- [40] C. Veaux, J. Yamagishi, and S. King, "The voice bank corpus: Design, collection and data analysis of a large regional accent speech database," in *IEEE International Conference Oriental COCOSA held jointly with 2013 Conference on Asian Spoken Language Research and Evaluation*, 2013, pp. 1–4.
- [41] J. Thiemann, N. Ito, and E. Vincent, "The diverse environments multi-channel acoustic noise database (demand): A database of multichannel environmental noise recordings," in *Proceedings of Meetings on Acoustics*, vol. 19, no. 1. AIP Publishing, 2013.
- [42] C.-C. Chiu, A. Narayanan, W. Han, R. Prabhavalkar, Y. Zhang, N. Jaitly, R. Pang, T. N. Sainath, P. Nguyen, L. Cao *et al.*, "Rnn-t models fail to generalize to out-of-domain audio: Causes and solutions," in *IEEE Spoken Language Technology Workshop*, 2021, pp. 873–880.
- [43] J. Kim and J. Lee, "Generalizing rnn-transducer to out-domain audio via sparse self-attention layers," in *INTERSPEECH*, 2022, pp. 4123–4127.
- [44] S. Long, Q. Zhou, X. Li, X. Lu, C. Ying, Y. Luo, L. Ma, and S. Yan, "Dgmamba: Domain generalization via generalized state space model," in *32nd ACM International Conference on Multimedia*, 2024, pp. 3607–3616.
- [45] A. Pandey and D. Wang, "On cross-corpus generalization of deep learning based speech enhancement," *IEEE/ACM Transactions on Audio, Speech, and Language Processing*, vol. 28, pp. 2489–2499, 2020.
- [46] P. Gonzalez, T. S. Alstrøm, and T. May, "Assessing the generalization gap of learning-based speech enhancement systems in noisy and reverberant environments," *IEEE/ACM Transactions on Audio, Speech, and Language Processing*, vol. 31, pp. 3390–3403, 2023.
- [47] B. Lenz, O. Lieber, A. Arazi, A. Bergman, A. Manevich, B. Peleg, B. Aviram, C. Almagor, C. Fridman, D. Padnos *et al.*, "Jamba: Hybrid transformer-mamba language models," in *The Thirteenth International Conference on Learning Representations*, 2025.
- [48] L. Ren, Y. Liu, Y. Lu, C. Liang, W. Chen *et al.*, "Samba: Simple hybrid state space models for efficient unlimited context language modeling," in *The Thirteenth International Conference on Learning Representations*, 2025.
- [49] Y. Fathullah, C. Wu, Y. Shangquan, J. Jia, W. Xiong, J. Mahadeokar, C. Liu, Y. Shi, O. Kalinli, M. Seltzer, and M. J. F. Gales, "Multi-head state space model for speech recognition," in *INTERSPEECH*, 2023, pp. 241–245.
- [50] D. Lee and J.-W. Choi, "Deft-mamba: Universal multichannel sound separation and polyphonic audio classification," in *IEEE International Conference on Acoustics, Speech and Signal Processing*, 2025, pp. 1–5.
- [51] Y. Sui, M. Zhao, J. Xia, X. Jiang, and S. Xia, "Tramba: A hybrid transformer and mamba architecture for practical audio and bone conduction speech super resolution and enhancement on mobile and wearable platforms," *Proceedings of the ACM on Interactive, Mobile, Wearable and Ubiquitous Technologies*, vol. 8, no. 4, pp. 1–29, 2024.
- [52] A. Pandey and D. Wang, "Self-attending rnn for speech enhancement to improve cross-corpus generalization," *IEEE/ACM Transactions on Audio, Speech, and Language Processing*, vol. 30, pp. 1374–1385, 2022.
- [53] C. K. Reddy, V. Gopal, R. Cutler, E. Beyrami, R. Cheng, H. Dubey, S. Matushevych, R. Aichner, A. Aazami, S. Braun, P. Rana, S. Srinivasan, and J. Gehrke, "The interspeech 2020 deep noise suppression challenge: Datasets, subjective testing framework, and challenge results," in *INTERSPEECH*, 2020, pp. 2492–2496.
- [54] J. Richter, Y.-C. Wu, S. Krenn, S. Welker, B. Lay, S. Watanabe, A. Richard, and T. Gerkmann, "Ears: An anechoic fullband speech dataset benchmarked for speech enhancement and dereverberation," in *INTERSPEECH*, 2024, pp. 4873–4877.
- [55] A. Gu, K. Goel, and C. Re, "Efficiently modeling long sequences with structured state spaces," in *International Conference on Learning Representations*, 2022.
- [56] D. Han, Z. Wang, Z. Xia, Y. Han, Y. Pu, C. Ge, J. Song, S. Song, B. Zheng, and G. Huang, "Demystify mamba in vision: A linear attention perspective," in *The Thirty-eighth Annual Conference on Neural Information Processing Systems*, 2024.
- [57] H. Zheng, Z. Yang, W. Liu, J. Liang, and Y. Li, "Improving deep neural networks using softplus units," in *IEEE International Joint Conference on Neural Networks*, 2015, pp. 1–4.
- [58] V. Panayotov, G. Chen, D. Povey, and S. Khudanpur, "Librispeech: An asr corpus based on public domain audio books," in *International Conference on Spoken Language Processing*, 2015, pp. 5206–5210.
- [59] Z.-H. Tan, N. Dehak *et al.*, "rvad: An unsupervised segment-based robust voice activity detection method," *Computer speech & language*, vol. 59, pp. 1–21, 2020.
- [60] J. H. Hansen and B. L. Pellom, "An effective quality evaluation protocol for speech enhancement algorithms," in *International Conference on Spoken Language Processing*, vol. 7. Citeseer, 1998, pp. 2819–2822.

- [61] G. Wichern, J. Antognini, M. Flynn, L. R. Zhu, E. McQuinn, D. Crow, E. Manilow, and J. L. Roux, “Wham!: Extending speech separation to noisy environments,” in *INTERSPEECH*, 2019, pp. 1368–1372.
- [62] International Telecommunication Union, “Recommendation ITU-R BS.1770-5: Algorithms to measure audio programme loudness and true-peak audio level,” <https://www.itu.int/rec/R-REC-BS.1770-5-202311-I/en>, 2023, [Online].
- [63] S. Wisdom, J. R. Hershey, K. Wilson, J. Thorpe, M. Chinen, B. Patton, and R. A. Saurous, “Differentiable consistency constraints for improved deep speech enhancement,” in *IEEE International Conference on Acoustics, Speech, and Signal Processing*, 2019, pp. 900–904.
- [64] A. Pandey and D. Wang, “Densely connected neural network with dilated convolutions for real-time speech enhancement in the time domain,” in *IEEE International Conference on Acoustics, Speech, and Signal Processing*, 2020, pp. 6629–6633.
- [65] K. He, X. Zhang, S. Ren, and J. Sun, “Delving deep into rectifiers: Surpassing human-level performance on imagenet classification,” in *IEEE International Conference on Computer Vision*, 2015, pp. 1026–1034.
- [66] Y. Ai and Z.-H. Ling, “Neural speech phase prediction based on parallel estimation architecture and anti-wrapping losses,” in *IEEE International Conference on Acoustics, Speech, and Signal Processing*, 2023, pp. 1–5.
- [67] V. Zadorozhnyy, Q. Ye, and K. Koishida, “Scp-gan: Self-correcting discriminator optimization for training consistency preserving metric gan on speech enhancement tasks,” in *INTERSPEECH*, 2023, pp. 2463–2467.
- [68] I. Loshchilov and F. Hutter, “Decoupled weight decay regularization,” in *International Conference on Learning Representations*, 2017.
- [69] A. W. Rix, J. G. Beerends, M. P. Hollier, and A. P. Hekstra, “Perceptual evaluation of speech quality (pesq)-a new method for speech quality assessment of telephone networks and codecs,” in *IEEE International Conference on Acoustics, Speech, and Signal Processing*, vol. 2, 2001, pp. 749–752.
- [70] J. Le Roux, S. Wisdom, H. Erdogan, and J. R. Hershey, “Sdr – half-baked or well done?” in *IEEE International Conference on Acoustics, Speech, and Signal Processing*, 2019, pp. 626–630.
- [71] J. Jensen and C. H. Taal, “An algorithm for predicting the intelligibility of speech masked by modulated noise maskers,” *IEEE/ACM Transactions on Audio, Speech, and Language Processing*, vol. 24, no. 11, pp. 2009–2022, 2016.
- [72] M. C. Cieslak, A. M. Castelfranco, V. Roncalli, P. H. Lenz, and D. K. Hartline, “t-distributed stochastic neighbor embedding (t-sne): A tool for eco-physiological transcriptomic analysis,” *Marine genomics*, vol. 51, p. 100723, 2020.
- [73] T. Dao, D. Fu, S. Ermon, A. Rudra, and C. Ré, “Flashattention: Fast and memory-efficient exact attention with io-awareness,” *Advances in Neural Information Processing Systems*, vol. 35, pp. 16 344–16 359, 2022.
- [74] T. Dao, “FlashAttention-2: Faster attention with better parallelism and work partitioning,” in *International Conference on Learning Representations*, 2024.
- [75] J. Shah, G. Bikshandi, Y. Zhang, V. Thakkar, P. Ramani, and T. Dao, “Flashattention-3: Fast and accurate attention with asynchrony and low-precision,” *Advances in Neural Information Processing Systems*, vol. 37, pp. 68 658–68 685, 2024.
- [76] S. Groot, Q. Chen, J. C. van Gemert, and C. Gao, “Cleanumamba: A compact mamba network for speech denoising using channel pruning,” in *IEEE International Symposium on Circuits and Systems*, 2025.
- [77] A. Pandey and D. Wang, “Dense cnn with self-attention for time-domain speech enhancement,” *IEEE/ACM Transactions on Audio, Speech, and Language Processing*, vol. 29, pp. 1270–1279, 2021.